IOP Conf. Series: Materials Science and Engineering **63** (2014) 012024 doi:10.1088/1757-899X/63/1/012024

Influence of composition, grain size, and oxide particles on the strength of consolidated ball-milled iron

J A Benito[1,2], V Gregoire[3,4], C Casas[2,3] and J M Cabrera[2,3]
[1] EUETIB, Universitat Politècnica de Catalunya, C/Comte d'Urgell 187, 08036 Barcelona, Spain.
[2] Fundació CTM Centre Tecnològic, Plaça de la ciencia 2, 08243 Manresa, Spain.
[3] ETSEIB, Universitat Politècnica de Catalunya, Av. Diagonal, 647, 08028 Barcelona, Spain.
[4] Eeigm, Université de Lorraine, 6 rue Bastien-Lepage CS, 10630, F-54010 Nancy, France.
E-mail: josep.a.benito@upc.edu

Abstract.
In this paper iron powders with two oxygen content (0.2 and 0.6% wt.) have been mechanically milled and consolidated by hot static pressing at different temperatures to obtain different grain sizes. At lower temperatures the grain size was in the nanostructured and ultrafine range and with increasing temperature abnormal grain growth was observed for both compositions. This led to the development of bimodal grain size distributions. In the samples with lower oxygen content the grain size and the percentage of coarse grain areas were larger than in the case of high oxygen content.
The strength and ductility have been determined by tensile tests. For low oxygen content, the presence of large coarse grains allowed plastic strain in some cases, and for the samples consolidated at higher temperatures, yield strength of 865 MPa with a 8% total strain were obtained. For the samples with high oxygen content plastic deformation was no possible in any case.
The observed stress for both compositions was analysed by two approaches, one based exclusively in grain boundary strengthening and the other one based in two effects acting at the same time: grain boundary and particle strengthening. Whereas grain boundary strengthening seems to fit with the strength of the samples in the nanostructured range, when coarse ferrite grains appear the addition of particle strengthening help to get better results. This indicates that the presence of oxides dissolved inside the large grains reinforce the structure of ball-milled iron.

1. Introduction

Mechanical milling of iron is a well-known method to get iron nanostructured powder [1-6]. One of the procedures to obtain a bulk material is consolidation at relatively high temperatures combined with the application of high pressures [2,6], rolling [3], or by spark plasma sintering (SPS) [5]. In all the cases certain contamination has been detected, coming from the grinding media or during consolidation process due to the high temperatures used. In this sense, the most common impurities are oxygen, carbon and chromium.
During the mechanical milling process, these elements are introduced inside the iron particles and there is a strong segregation into the grain boundaries of the formed nanocrystalline ferrite [5,7]. At the same time, a part of these atoms are solved inside the ferrite grains. In the case of interstitials as carbon, its presence is related to the blocking of dislocations [8]. In the case of fine particles as oxides, its presence is related to an additional strengthening of the mechanically milled powder [9].
The presence of these alloying elements involves an increase of hardness in the milled powder and also greater difficulties in consolidation. As a consequence, ball-milled iron is a high strength material that shows brittle behavior in tensile tests [1,2,6,10], although in compression test larger strains have been obtained [5,11]. In the latter, the presence of a bimodal grain size distribution with large coarse grains it seems to help uniform deformation.

It was confirmed when ball-milled iron was consolidated via SPS with bimodal grain size distributions since high strength with reasonable ductility in tensile tests was observed [5].
It is also worth mentioning that the alloying elements play a role in the strengthening mechanisms of ball-milled iron. In this material high particle strengthening has been related to the presence of atoms and particles dispersed in the ferrite grains. This mechanism could be as important as grain boundary strengthening [9]. Nevertheless, for low-oxygen content irons in the nanostructured range the grain boundary strengthening is capable to explain their strength by the use of usual Hall-Petch equations used for ultrafine IF steels [12].
In the present paper ball milled iron with two oxygen compositions have been consolidated by hot static pressing with the aim to know if the development of bimodal grain size distribution can help to obtain high strength with moderate ductility. In parallel, the study of microstructure and the different oxygen composition can be useful to understand the role of oxide particles in the strength of nanostructured and ultrafine ball-milled iron.

2. Experimental procedure

Commercial pure iron powder with a particle size between 75 and 160 μm was used as a starting material. In order to obtain two different oxygen compositions, one of the millings was carried out introducing 6g of iron in the vials (series A). In the other one 0.06 g of Fe_2O_3 were added to the 6 g of iron (series B). Mechanical milling was carried out under gas atmosphere for 17 hours in a planetary ball mill using 250 cm^3 stainless steels vials with 75 mm of inner diameter. 40 balls of 10 mm diameter made of hardened steel 100Cr6 were used. The ratio balls-powder was 27:1.
The milled powder was consolidated by a hot static compaction at a fixed pressure of 510 MPa held for 1 hour. Different temperatures were used from 500 to 650 ºC. The specimens were 1 mm in height and 10 mm in diameter. In the present work no wax was used to help the compressing of the powder due to its high carbon content. The table 1 shows the chemical composition of the initial iron powder and the final composition of the two series of the consolidated samples. For the chemical analysis different techniques were used. For the determination of metals content spark emission spectrometry was used. The carbon content was determined by combustion gas analysis and inert gas fusion was used to obtain the oxygen and nitrogen content. In the two series of consolidated specimens contamination from grinding media is observed, especially Cr and Ni. Moreover, in both series there was an increase of oxygen and carbon with respect to the initial material. In the series B the addition of oxide powder has led to higher levels of both elements. The hardness for every consolidated sample was evaluated by Vickers indentations on the flat sides of the samples with a load of 2 kN.

Table 1. Composition in wt.% of initial powder and the two series of consolidated specimens (Fe. Balance).

	O	C	P	N	Cr	Ni	Si	Mn
Initial	0.110	0.010	0.010	-	-	-	0.010	0.106
Series A	0.238	0.026	0.011	0.018	0.946	0.498	0.028	0.220
Series B	0.634	0.087	0.011	0.028	0.954	0.503	0.031	0.216

Specimens for tensile tests were cut from the consolidated samples using wire electrical discharge machining. No tensile specimens were obtained from the samples consolidated at 500 ºC since brittle behavior with very low strength was expected. The specimens were 1 mm wide, 0,8-1 mm thick and 3 mm of gage length. Tensile tests were conducted in a Deben tensile machine at an initial strain rate of $1.7 \cdot 10^{-3}$ s^{-1}.
The microstructural analysis was performed using a Field Emission Scanning Electron Microscopy (FESEM) using a JEOL JSM6400 microscope. The grain size was determined from SEM images using ASTM-E112 methodology. For every micrograph the grain

boundaries of ferrite were enhanced and the resulting image introduced in the image analyzer software *Omnimet* for the calculation of grain size. In order to differentiate areas of nano or ultrafine grains from areas of coarse grains in bimodal structures, grains with diameter lower than 500 nm were considered as nano or ultrafine grains, whereas larger grains were computed as coarse grains.

3. Results

3.1. Microstructure

The evolution of the microstructure with temperature for both irons is exposed in Fig.1. The values of grain size for the fine grained and coarse grains areas together with the volume fraction of coarse grain areas are displayed in Table 2. In this table a calculated mean grain size for every series (D_A and D_B) is also exposed.

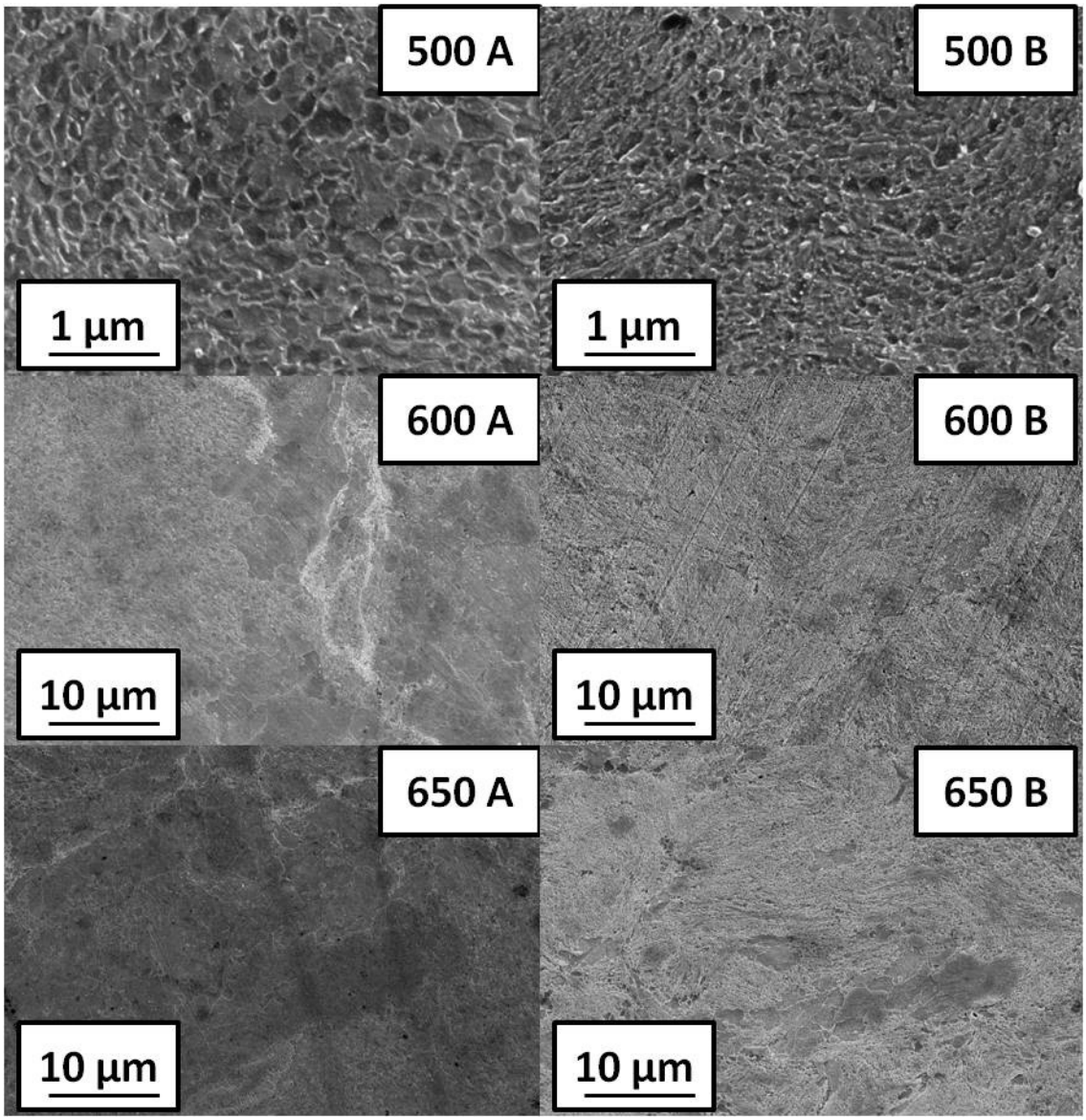

Fig. 1. Field Emission Scanning Electron Microscopy (FESEM) images. Secondary electron images showing the evolution of the microstructure of the consolidated samples for series A and B with temperature at 500, 600 and 650 ºC.

The presence of oxygen and carbon atoms in the ball-milled microstructure leads to the formation of oxides and carbides. In the present case, due to the high chromium content, it has been found that the oxides could be $FeCr_2O_4$ and Fe_3O_4 [5]. These oxides and carbides are preferentially located in the grain boundaries of the nanostructured powder [5,7]. During the consolidation process at high temperatures these particles act as pinning points for grain boundaries and consequently the grain growth is delayed. When the grain boundaries finally move, most of these particles are finally trapped inside the new ultrafine or larger grains [5,13]. As a consequence of this, for the series A with lower oxygen and carbon content the grain size is larger than for series B at any temperature.

Table 2. Grain size for series A and B as determined from FESEM images.

T (°C)	Series A (0.24% O)				Series B (0.63% O)			
	Grain size (μm)		Volume fraction of coarse grains (%)	Mean grain size (μm) (D_A)	Grain size (μm)		Volume fraction of coarse grains (%)	Mean grain size (μm) (D_B)
	Fine	Coarse						
500	0.16	-	-	0.16	0.09	-	-	0.09
575	0.23	1.38	38	0.67	0.15	1.04	2	0.16
600	0.24	1.77	34	0.76	0.18	1.20	6	0.24
625	0.25	1.75	46	1.00	0.16	1.44	21	0.43
650	0.28	1.79	54	1.09	0.20	1.35	17	0.39

As expected, consolidation at 500 ºC rendered very fine ferrite grain size in both series, without abnormal grain growth. However, at 575 ºC, for series A large zones of coarse ferrite grains were found. With higher temperatures, a slight increase of these coarse grained areas was found. At the same time, the fine grained areas were capable of retain low grain size values. In the case of series B, the onset of a bimodal grain size distribution was delayed until the samples consolidated at 625 ºC and 650 ºC, in which the percentage of coarse grains reached values around 20 %. In fact, in order to achieve percentages of coarse grain zones similar to series A, the consolidation temperature should have been still higher.

3.2. Tensile tests

The figure 2 shows the stress-strain curves for the both series of consolidated ball-milled iron. For the series B with higher oxygen content the samples broke with no plastic deformation. Moreover, except the samples consolidated at 650 ºC, the strength was clearly below the expected values after hardness measurements. For 650 ºC samples, σ_y was 1430 MPa and total strain was slightly above 1%. For this series, it is clear that only at 650 ºC the metallurgical bonding between former powder particles was enough good. This fragile behavior of the series B can be explained by the high hardness of iron powders with a large oxygen and carbon content [14].

For the series A, all the samples tested gave yield strengths close to the prediction after hardness measurements. It is a sign that indicates that the bonding between particles was good. However, ductility was rather poor in all the cases except for the case of 650 ºC. We can explain this behavior since in this case no wax was used in order to facilitate the compressing of ball-milled powder, and this probably has led to a moderate presence of artifacts in the

bulk materials. In addition, it has been shown that the fracture toughness of ultrafine grained iron can be very low [15]. Therefore, samples consolidated at 575 and 600 ºC showed only a 1% strain although the percentage of coarse grain zones was above 30%. For the case of 625 ºC, a transition to brittle to more ductile behavior was observed. Finally, 650 ºC samples showed around 4-5% uniform deformation with a slight strain hardening. This strain hardening has been attributed to the role of coarse grains which are capable of storing dislocations. The total strain reached the 8% in the best case.

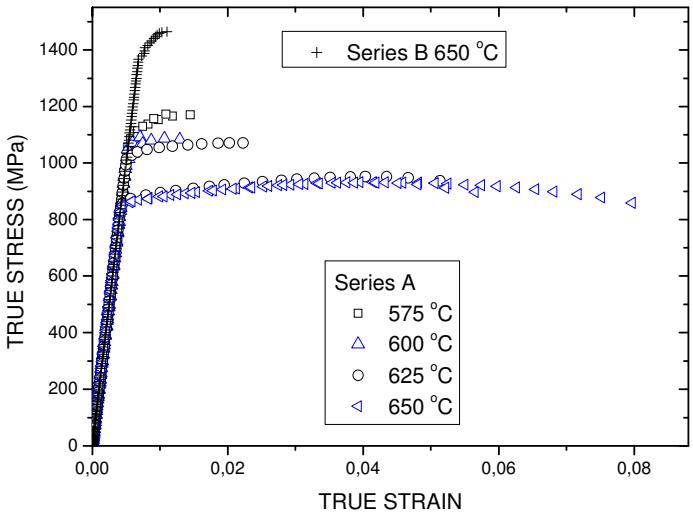

Fig. 2. Tensile stress-strain curves for the series A and B.

3.3. Analysis of strength

As mentioned in the introduction, the analysis of the yield strength (σ_y) of the consolidated ball milled iron with oxygen and carbon content can be evaluated using two approaches. In the first one, it can be considered that the strengthening mechanism is mainly controlled by grain boundaries. In this case, we can make a prediction using the well-known Hall-Petch relationship $\sigma_y = \sigma_o + k_y \cdot D^{-1/2}$. Where σ_o, and k_y are the friction stress and the Hall-Petch coefficient k_y, respectively. For k_y, the value associated for iron changes from 150 MPa·μm$^{-1/2}$ to 600 MPa·μm$^{1/2}$ depending on the carbon content [16]. The presence of only 60 ppm of carbon rises to 600 MPa·μm$^{1/2}$ and this value seems to work well for grain sizes below 1 μm [12]. Therefore, this value has been taken here for k_y. With regard σ_o, it has been determined that the presence of Cr and P increases the friction stress of iron [17]. The calculations with the present content of Cr and P resulted close to the value reported be Takaki et al, 100 MPa. Therefore, in the prediction of yield strength (σ_{yP}) by grain boundary strengthening the Eq(1) will be used.

$$\sigma_{yP} = 100 + 600 \cdot D^{-1/2} \qquad \text{Eq(1).}$$

In the second approach, it can be considered that the oxide particles present in the microstructure play a role in the overall strengthening of the bulk specimens. Lesuer et al.proposed a model in which a term called particle strengthening (σ_P) was added to the Hall-Petch relationship [9]. In this case, the friction stress will be considered the same that in the first approach and the coefficient k_y related to grain boundary strengthening is reduced to 260 MPa·μm$^{-1/2}$ [9]. With regard to particle strengthening, $\sigma_P = B \cdot D_s^{-1/2}$, where D_s is the interparticle spacing and B is a constant with a reported value of 395 MPa·μm$^{1/2}$. The interparticle spacing D_s is related to the volume fraction and average diameter of the oxides

solved in the ferritic matrix. In this work this information has not been yet obtained and according to Lesuer et al, the value of D_s will be estimated from the grain size (D) of every sample using D_s=0.4·D. Therefore, in the prediction of yield strength (σ_{yP}) by grain boundary strengthening and particle strengthening the Eq(2) will be used:

$$\sigma_{yP} = 100 + 260 \cdot D^{-1/2} + 395 \cdot (0.4D)^{-1/2} \qquad \text{Eq(2).}$$

It is important to mention here that there are some differences between the ball-milled iron described in the model by Lesuer et al and the present ball milled iron. The most important is the milling time, since in the present case the powder was milled for 17 hours, well below the estimated time to develop a structure dominated by high angle boundaries, around 100 hours. In addition, longer milling times would help to disperse more effectively the oxides inside ferritic matrix and the strengthening would be greater. However, recent studies with consolidated samples of ball-milled iron with a 0.39 % oxygen content, have shown that even with milling time below 20 hours the structure is mainly formed by high angle boundaries [18]. Therefore, it is considered that the strength of the present ball-milled iron can be evaluated by the model developed by Lesuer et al.
In the figure 3 the experimental yield strengths (σ_y) for both series are plotted with the predicted yield strength (σ_{yP}) by the two approaches. For the analysis of strength for the samples consolidated at 500 ºC and for the samples in series B in which it was no possible to determine the yield strength by tensile test due to its fragile behavior, the hardness values were converted to yield strength by Hv=3 σ_y.

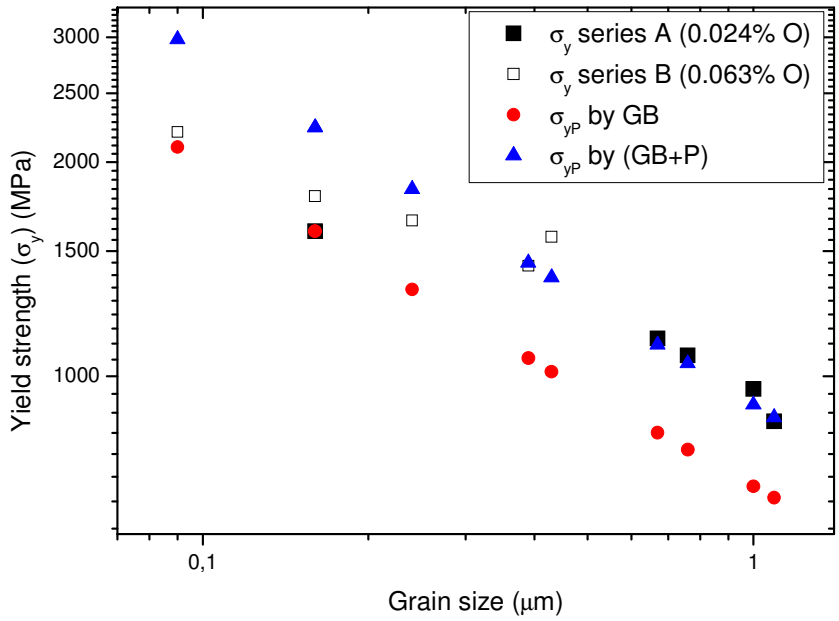

Fig.3. Experimental yield strength (σ_y) for series A and B with mean grain size. Predicted yield strength (σ_{yP}) by grain boundary strengthening (GB) and by a combined model between grain boundary and particle strengthening (GB+P).

In the nanostructured range, the strength for the series A and B fit reasonably well with Eq(1). For the series A there is no difference between the experimental and the predicted values. For the series B with higher oxygen content the predicted values are close but slightly above the real ones. It seems that for nanocrystalline ferrite the grain boundary strengthening allows to explain the strength of ball-milled iron since in this range the oxides

would be located mainly in the grain boundaries [5,7]. Nevertheless, it must be pointed out that in the case of series B, with 0.63% wt.O, the small increase in strength for samples consolidated at 500 and 575 ºC with respect to Eq(1) could be related to a small presence of oxides solved inside the grains. Especially for 575 ºC samples, with a mean grain size of 0.16 μm.

At the time that some grain growth is observed, a gradual deviation of the experimental values from the predictions by Eq (1) is found. In the case of series B, in which the coarsening of grains was slower, a clear transition is observed. When the percentage of coarse grains is rising but below the 20%, the predicted values lie between both approaches. For samples in which this percentage reaches 20%, the predictions of Eq(2) fit to the experimental values. For series A, in which there is no transition between nanostructured range and clear bimodal grain size distributions, the experimental values move from the fitting line to Eq (1) to the fitting line to Eq(2). In both cases, strengthening from the fine oxide that now is well inside the ultrafine and coarse grains it seems to be acting in addition to grain boundary strengthening. It is important to point out that the estimation of interparticle spacing D_s works rather well especially for series A.

4.Conclusions

In the nanostructured range the strength of ball-milled iron of different oxygen content was reasonably explained by grain boundary strengthening, although for high oxygen compositions (0.63%wt.) some additional strengthening was observed.

For ball-milled iron with bimodal grain size distribution, the predicted values using a combination of grain boundary strengthening and particle strengthening allowed to explain the strength of the consolidated samples.

For the consolidated samples with a low oxygen content (0,24% wt.) good combination of strength and ductility was observed, whereas for samples with higher oxygen content (0.63%) high strength but lack of ductility was observed at the consolidation temperatures used.

5. References

[1] Mallow T R et al 1998 *Mater. Sci. and Eng. A* **252** 36.
[2] Jia D et al 2003 *Acta Mater.* **51** 3495
[3] Belyakov A et al 2003 *Scripta Mater.* **48** 1111.
[4] Kimura et al 2000 In: Symposium on ultrafine grained materials at the 2000 TMS annual meeting, Edited by the minerals, metals and materials society. 277-286
[5] Srinivasarao B et al 2009 *Acta Mater.* **57** 3277.
[6] Tejedor R et al 2008 *Scripta Mater.* **59** 631.
[7] Ohsaki S et al 2005 *Scripta Mater.* **52** 271.
[8].Sauvage X et al 2007 *J of Mater. Sci.* **42** 1615.
[9].Lesuer et al 2006 *Mater. Trans.* **47** 1508.
[10] Cheng S et al 2008 *Mat. Sci. and Eng. A* **493** 226.
[11] Benito J A et al 2008 *Mat. Sci. Forum* **584-586** 617.
[12] Takaki S 2012 *Mat. Sci. Forum* **706-709** 181
[13] Belyakov A et al 2004 *Mater. Trans.* **45** 2252.
[14] Rodriguez-Baracaldo et al 2008 *Mat. Sci. and Eng. A* **493** 215.
[15] Hohenwarter et al 2010 *Mat. Sci. and Eng. A* **527** 2649.
[16] Takeda et al 2008 *ISIJ Inter.* **48** 1122.
[17] Takaki S 2010 *Mat. Sci. Forum* **638-642** 168.
[18] Benito J A et al, submitted to publication.